THE DIFFRACTION OF AN UNDERWATER SHOCK WAVE BY A SEMI-INFINITE PLANE.

Leif Bjørnø
Department of Fluid Mechanics
The Technical University of Denmark, Lyngby, Denmark.

Abstract.

A great number of pressure-time curves measured in shock waves arising from underwater explosions show the existence of a well-defined pressure "shadow and light region", bounded by a strong pressure gradient between the two regions, at the diffraction of the shock waves by a semi-infinite plane situated in the entrance from a channel into a water-filled tank. Through the modification of a method for direct solution of the diffraction problems by pressure waves in air, introduced by Friedlander, it has turned out to be possible to extend the method also to comprise the calculation of the pressure variation in the wave system arisen by diffraction of weak underwater shocks. A good accordance between the theoretical and the experimental values have been stated.

Introduction.

During the last 7o years an increasing number of papers treating the diffraction of a pulse by wedges and half-planes have been published. Sommerfeld's [1] exact solution to diffraction of a simple harmonic wave train by a straight-edged semi-infinite screen obtained by his application of the method of images on a Riemann surface, was 19o1 extended by himself [2] to cover the diffraction of a rectangular pulse.

The pulse diffraction problem was later treated by Lamb [3], who came to a solution on a form different from the one of Sommerfeld. As shown by Friedlander [4] the two forms can be brought in accordance with each other by a transformation. A bibliography of some of the most essential works on the diffraction of sound pulses can be found in [5] together with a thorough exposition of the theory of diffraction.

In an early stage of the development it was obvious that even if the case of pulse diffraction and the case of diffraction of infinite trains of simple harmonic waves are analogous, they differ in several respects. The different nature of the physical phenomena

in the two cases for instance causes different types of equations governing their propagation.

Early attempts by application of Fourier transforms to extend the results from the diffraction of simple harmonic waves to cover the diffraction of pulses had demonstrated the inaccuracy of the obtained results. This further emphasized the necessity of a direct solution to the pulse diffraction problems, but very few general or approximate methods are available, the approximate methods only apply to limited frequency ranges. Such a general method, giving a direct solution to the problem of diffraction of a sound pulse of arbitrary shape by a semi-infinite plane, can be found in [4].

Another aspect of the pulse diffraction problem includes the diffraction of shock waves by corners and semi-infinite planes. In this connection literature shows gases to be the medium preferred for the investigations while shock waves in water have not yet been treated in connection to diffraction of pulses.

M. J. Lighthill [6], [7], linearised the two-dimensional problem of diffraction of blast waves of arbitrary strength by a small-angle corner. Diffraction of shock waves in air by corners of an arbitrary angle was investigated by G. B. Whitham [8], who used an approximate theory in which the disturbances to the flow are treated as a wave propagation on the shocks. The work can be considered as a generalisation to shock waves of the theory of geometrical acoustics, which for weak shocks leads to some discrepancy because the approximate theory concentrates the change in Mach-number over a relatively small part of the shock.

A review of some recent works on shock wave diffraction over compression and expansion corners in gases is given by R. R. Meynants [9], together with a comparison of results from a number of shock tube experiments.

In the present work an attempt is made to modify and to extend the theory of diffraction of sound pulses put up in [4] to cover the diffraction of weak shock waves in water by a semi-infinite plane.

A direct solution to the diffraction problem.

Let us consider the diffraction of a plane pressure pulse with a small amplitude incident upon a semi-infinite plane, see figure 1. The pulse front assumes parallel to the semi-infinite plane, which is supposed to be completely reflecting.

Choosing a coordinate system (see figure 1) with the z-axis along

the edge of the semi-infinite plane, which occupies the lower (positive x) part of the x-z-plane, the plane diffraction problem will depend on the variables x, y and t.

By the calculation it will be appropriate to introduce parabolic coordinates.

$$x + iy = (\xi + i\eta)^2, \quad \text{where} \quad \eta \geq 0 \tag{1}$$

by which

$$x = \xi^2 - \eta^2 \quad \text{and} \quad y = 2\xi\eta$$

Hereby the x-y-plane is transformed into the upper half of the ξ-η-plane, while the positive part of the x-axis (the trace of the semi-infinite plane in the x-y-plane) transforms into the whole ξ-axis.

Is the existence of a velocity potential ϕ assumed, it satisfies the wave equation:

$$\frac{\partial^2\phi}{\partial x^2} + \frac{\partial^2\phi}{\partial y^2} = \frac{1}{c^2}\frac{\partial^2\phi}{\partial t^2} \tag{2}$$

where c is the sound velocity.

The boundary condition at the semi-infinite plane must be:

$$\frac{\partial\phi}{\partial y} = 0 \quad \text{for } (x \geq 0,\ y = 0) \quad \text{or} \quad \frac{\partial\phi}{\partial\eta} = 0 \quad \text{for} \quad (\eta = 0) \tag{3}$$

The velocity potential for the incident plane wave (pulse) at figure 1 can by means of (1) and (2) generally be written:

$$\phi = F(ct + y) = F(ct + 2\xi\eta) = F(z) \tag{4}$$

where $F(z) = 0$ for $z \leq 0$

A solution for (2) which at the same time satisfies the boundary conditions by the semi-infinite plane and at infinity is given in [9] :

$$\phi = \tfrac{1}{2}F(ct + 2\xi\eta) + \tfrac{1}{2}F(ct - 2\xi\eta) + \int_0^{\xi+\eta} f(ct + 2\xi\eta - \zeta^2)d + \int_0^{\xi-\eta} f(ct - 2\xi\eta - \zeta^2)d\zeta \tag{5}$$

The function f( ) will be determined later.

$$x \to -\infty \text{ leads to } \phi = F(ct + 2\xi\eta) \tag{6}$$

the semi-infinite plane not having any influence on the wave far

from the edge of the plane.

By (1), (5) and (6) give for $x \to -\infty$

$$\tfrac{1}{2}F(ct + 2\xi\eta) - \int_0^{\infty} f(ct + 2\xi\eta - \zeta^2)d\zeta = \tfrac{1}{2}F(ct - 2\xi\eta) - \int_0^{\infty} f(ct - 2\xi\eta - \zeta^2)d\zeta \qquad (7)$$

While (7) must be satisfied for $\eta \to \infty$ together with $t = 0$ and $\xi = 0$, f must satisfy the integral equation:

$$\tfrac{1}{2}F(z) - \int_0^{\infty} f(z - \zeta^2)d\zeta = 0 \qquad (8)$$

The introduction of the substitution:

$$z - \zeta^2 = u \quad \text{and} \quad d\zeta = \frac{-du}{2\sqrt{z - u}} \qquad (9)$$

in (8) leads to:

$$\int_{-\infty}^{z} \frac{f(u)\,du}{\sqrt{z - u}} = F(z) \qquad (10)$$

Further, if $\lim_{z \to \infty} F(z) = 0$ (11)

is assumed, the function f( ) according to [10] can be found of (10) as:

$$f(u) = \frac{1}{\pi}\int_{-\infty}^{u} \frac{F'(z)dz}{\sqrt{u - z}} \qquad (12)$$

As the incident pulse in according to (4) is assumed to have a definite wave front, (10) and (12) can be written as:

$$F(z) = \int_0^{z} \frac{f(u)du}{\sqrt{z - u}} \quad (10a) \quad \text{and} \quad f(u) = \frac{1}{\pi}\int_0^{u} \frac{F'(z)dz}{\sqrt{u - z}} \qquad (12a)$$

Integration by parts of (12a) leads to:

$$f(u) = \frac{1}{\pi}\left[2\sqrt{u}\,F'(0) + 2\int_0^u \sqrt{u-z}\,F''(z)dz\right] \tag{13}$$

from which:

$$f'(u) = \frac{F'(0)}{\pi\sqrt{u}} + \frac{1}{\pi}\int_0^u \frac{F''(z)dz}{\sqrt{u-z}} \tag{14}$$

As the pressure is the parameter which easiest can be measured by a shock wave from an underwater explosion, the pressure variation by diffraction around the semi-infinite plane will especially be emphasized in the following.

By the velocity potential ϕ the pressure (excess pressure over hydrostatic) can be found from:

$$p = \rho\frac{\partial\phi}{\partial t} \tag{15}$$

where ρ is the fluid density.

With reference to the equation (5), (15) leads to:

$$p = \rho c\left[\tfrac{1}{2}F'(ct + 2\xi\eta) + \tfrac{1}{2}F'(ct - 2\xi\eta) + \int_0^{\xi+\eta} f'(ct + 2\xi\eta - \zeta^2)d\zeta + \int_0^{\xi-\eta} f'(ct - 2\xi\eta - \zeta^2)d\zeta\right] \tag{16}$$

Introducing the substitution:

$$v(u) = \rho c f'(u) \quad \text{and} \quad p_o(z) = \rho c F'(z) \tag{17}$$

where $p_o(z)$ is the pressure function in the incident pulse, (14) and (16) can be written:

$$v(u) = \frac{p_o(0)}{\pi\sqrt{u}} + \frac{1}{\pi}\int_0^u \frac{p_o'(z)dz}{\sqrt{u-z}} \tag{14a}$$

and

$$p = \tfrac{1}{2}p_o(ct + 2\xi\eta) + \tfrac{1}{2}p_o(ct - 2\xi\eta) + \int_0^{\xi+\eta} \psi(ct + 2\xi\eta - \zeta^2)d\zeta + \int_0^{\xi-\eta} \psi(ct - 2\xi\eta - \zeta^2)d\zeta \qquad (16a)$$

The equations (14a) and (16a) determine the pressure function in the wave system arising from the diffraction of the incident plane pulse by the reflecting semi-infinite plane. On basis of the knowledge of the pressure function $p_o(z)$ and the derivative $p_o'(z)$ in the incident pulse, the function $\psi(u)$ leading to p can be determined.

By means of (10a) and (17)

$$p_o(z) = \int_0^z \frac{\psi(u)du}{\sqrt{z - u}} \qquad (18)$$

can be found.

Returning to the original x-y-coordinate system the pressure function p in the three regions given on figure 1, by means of (18) can be written:

$$p_1 = p_o(ct + y) + p_o(ct - y) - I_1 - I_2$$

$$p_2 = p_o(ct + y) - I_1 + I_2 \qquad (19)$$

$$p_3 = I_1 + I_2$$

where:

$$I_1 = \int_0^{(ct+y)^{\frac{1}{2}}} \frac{\psi(ct + y - \zeta^2)d\zeta}{((x^2+y^2)^{\frac{1}{2}} + y)^{\frac{1}{2}}} \quad \text{and} \quad I_2 = \int_0^{(ct-y)^{\frac{1}{2}}} \frac{\psi(ct - y - \zeta^2)d\zeta}{((x^2+y^2)^{\frac{1}{2}} - y)^{\frac{1}{2}}}$$

By a suitably chosen substitution the integrals I_1 and I_2 can be written:

$$I_1 = \tfrac{1}{2}\int_0^{ct-(x^2+y^2)^{\frac{1}{2}}} \frac{\psi(u)du}{\sqrt{ct + y - u}} \quad \text{and} \quad I_2 = \tfrac{1}{2}\int_0^{ct-(x^2+y^2)^{\frac{1}{2}}} \frac{\psi(u)du}{\sqrt{ct - y - u}} \qquad (20)$$

With reference to a numerical treatment of the expressions found

for the pressure variation the following substitutions are introduced:

$$X_1 = (x^2 + y^2)^{\frac{1}{2}} + y, \quad X_2 = (x^2 + y^2)^{\frac{1}{2}} - y,$$
$$T = ct - (x^2 + y^2)^{\frac{1}{2}}. \tag{21}$$

By use of (14a), (2o) and (21) the following expression can be found:

$$P(X,T) = \frac{\sqrt{X}}{\pi} \int_0^T \frac{p_o(z)\, dz}{(T + X - z)^{\frac{1}{2}} (T - z)^{\frac{1}{2}}} \tag{22}$$

The pressure variation in the three regions on figure 1 can now be obtained from (19) as:

$$p_1 = p_o(ct + y) + p_o(ct - y) - \tfrac{1}{2}\left[P(X_1,T) + P(X_2,T)\right]$$
$$p_2 = p_o(ct + y) - \tfrac{1}{2}\left[P(X_1,T) - P(X_2,T)\right] \tag{23}$$
$$p_3 = \tfrac{1}{2}\left[P(X_1,T) + P(X_2,T)\right]$$

<u>The theory of diffraction applied to the shock wave from an underwater explosion.</u>

As shown in [11] the pressure variation as a function of time and space behind the front of a shock wave from an underwater explosion can be written:

$$p_o(z') = p_{mo} e^{-z'} \qquad \text{for } z' \geq 0 \tag{24}$$

and

$$p_o(z') = 0 \qquad \text{for } z' < 0$$

where

z' : the dimensionless substitution $= \dfrac{ct + y}{c\theta}$

θ : time constant in the exponential pressure decay behind the shock front.

p_{mo} : peak pressure in the incident shock wave.

An introduction of the dimensionless pressure variation $p_o(z)/p_{mo}$ in the expression (22) leads to:

$$P(X,T) = \frac{\sqrt{X}}{\pi} \int_0^T \frac{e^{-z'} dz'}{(T + X - z')(T - z')^{\frac{1}{2}}}$$

which by the substitution $z' = T - u^2$ and $dz' = -2udu$ gives the result:

$$P(X,T) = \frac{2\sqrt{X}}{\pi} e^{-T} \int_0^{\sqrt{T}} \frac{(e^{u^2})\, du}{X + u^2} \qquad (25)$$

Together with p_2 and p_3 from (23) the expression (25) forms the basis of the numerical calculation of the pressure variation in the "light region" (region 2 on figure 1) and the "shadow region" (region 3 on figure 1) by the diffraction of the shock wave.

As shown in [4] the pressure variation in the wave front across the "shadow boundary" (the negative part of the y-axis) will be discontinuous if the incident shock wave is given a discontinuity in the front.

Such a discontinuity will be physically irrealistic, and as shown in [11] a shock wave from an underwater explosion will be continuous in pressure variation with a finite rise-time to the peak pressure.

Therefore the pressure variation expressed by (24) will only be valid after the peak pressure obtained.

Previous measurements [11] and [12] have shown a rise-time at about 1 µsec. which, therefore, have formed the basis of the numerical calculations. The curves calculated for the variation in peak pressure for the diffracted shock wave across the shadow boundary therefore becomes continuous.

Curves for the dimensionless peak pressure variation across the shadow boundary for fixed y-values, y = -1oo mm, y = -4oo mm, y = -7oo mm and y = -1ooo mm respectively, with sign given in accordance to figure 1, are shown on the figures 3 - 6. On the figures p_m designates the peak pressure in the shock wave after the diffraction.

A comparison between a calculated and an experimentally found pressure-time variation for fixed coordinates (x,y) = (5o mm, -1oo mm) in the shadow region is shown on figure 7.

Experimental arrangement.

The measurements took place in a water tank immediately after the outled from a water-filled channel. The dimensions of the tank were 2 x 2 x 2 m. The length of the channel was 5 m and its cross dimensions were 600 x 700 mm. The tank side had a prolongation of 50 mm into the cross section of the channel, which formed the semi-infinite plane, see figure 2.

The explosions took place in the channel in a distance varying from 2,5 to 4,5 m from the outled to the tank.

Detonators (Nobel Dynamite, typ.6) with a total explosive charge equivalent to 0,8 g TNT were used as shock wave generators.

An excellent reproduceability by the shock waves from this type of detonators has been demonstrated by previous experiments [11].

The measurements of the pressure-time curves by the wave systems in the light and shadow region were carried out by means of turmaline transducers (marked: Crystal Research Inc. Mass. U.S.A.) with the dimensions 1/4" and 1/8".

The transducers had a sufficient sensitivity in order to be directly connected to the entrance of an oscilloscope (marked: Tektronix 555), even by measurements deeper inside the shadow region. The signal/noise ratio did not allow a measurement in the shadow region closer than y = - 100 mm from the channel outled.

By means of U-formed sectional iron a slide system was formed to place the transducer in the right position. The slide system caused a total accuracy of $\pm$6,5 mm for the y-coordinates and of $\pm$3,4 mm for the x-coordinates at a distance y = - 1000 mm.

The uncertainty mentioned on the transducer coordinates gets the greatest contribution from the deviation in the detonator coordinates between each shot.

The uncertainties by the coordinate determination leads together with the registration uncertainty to a relative uncertainty of less than 4% at the pressure measurements.

The assumption, that the incident shock wave should be plane, is a good approximation. Inside the relatively small x-dimensions compared to the greater radial distances from the detonation, which were of interest during the experiments, the shock wave can by all means be considered as plane, in spite of the spherical character of the shock waves from underwater explosions ($p_{mo} \sim R^{-1,1}$).

Modifications in the peak pressure p_{mo} and the time constant θ of

the shock wave as a function of the distance R from the detonation were corrected for every y-position before the calculation of the variation in the dimensionless pressure ratio across the shadow boundary.

The assumption of small amplitudes in the incident shock wave is satisfied with the measured peak pressures of about 14 bar (over hydrostatic pressure), which according to [11] leads to a variation in density of less than 1 per thousand of the water density in front of the shock wave. The particle velocity in the shock front will under this condition be below 1 per thousand of the shock velocity or the sound velocity.

Stronger shock waves may be expected to give greater deviations from the theoretically calculated values, the shock velocity in this case not being considered as constant and the non-linear properties of the shock will be more prevalent. Previous measurements [11] have shown that peak pressures at about loo bar only will lead to a shock velocity which deviates less than 1% from the sound velocity in the undisturbed water in front of the shock.

Experimental results.

The figures 3 to 6 show a comparison between the theoretically prescribed and the experimentally found variations in the dimensionless peak pressure of the waves across the shadow boundary for different y-values.

Both the measurements and the theory confirm the geometrical shadow boundary as a line through the points in which the peak pressure is the half of the peak pressure p_{mo} of the undisturbed shock wave (measured directly in the light region). The experimental curves are drawn from the measured dimensionless peak pressures by the employment of the method of least squares. Further, the strong gradient in peak pressure in the x-direction across the shadow boundary is noted, which at y = -loo mm shows a pressure decay at about 6o% within 4o mm. The same gradients decreases with increasing (negative) y in order by y = -looo mm to show a pressure decay of 6o% across about 2oo mm. The strong gradient is among other things supposed to be due to the shock character of the wave, described by the short rise-time.

The course of the theoretically found and the measured curves show a good accordance in the shadow region, apart from the course at y = - loo mm. The extremely weak signals for x > 9o mm in the

shadow region at y = -loo mm prevented an accurate determination of the pressure variation.

Further the measurements in the shadow region show a systematical tendency, that the measured pressure values at the same x-coordinate should increase faster than the calculated pressure values by increasing distances in y. The agreement between the calculated and the measured values at the shadow boundary and in greater distances from it seems to be a reality in spite of relative movements of the intermediate values.

No systematic relative movement of the two curves seems to appear in the light region. Also here a fair agreement between theory and experiment is obtained although the influence of diffraction on the incident shock wave seem to appear further into the light region, than prescribed by the theory. This might derive from non-linearities in connection to the interaction between the diffracted wave and the shock wave, a circumstance not considered in the theory.

The calculations and the measurements show that the rise-time of the wave increases with increasing x-values in the shadow region, leading to a displacement of the energy-spectre towards lower frequencies. Thus figure 7 shows the calculated and the measured dimensionless pressure-time variation at the position (x,y) = (5o mm, -loo mm), where the peak pressure is not obtained until about 9 µsec after the wave front.

The course of the two curves seems to underline the applicability of the method of direct solution by the calculation of the diffraction of weak shock waves.

Conclusion.

The theory and the measurements have shown the existence of a well-defined light and shadow region in pressure bounded by a relatively sharp peak pressure gradient across the geometrical shadow boundary. The fair agreement between the theoretically calculated and the experimentally found values in varying distances behind the semi-infinite plane seems to support the applicability of the method of direct solution and also to extend the method to comprise the diffraction of weak underwater shock waves by a semi-infinite plane.

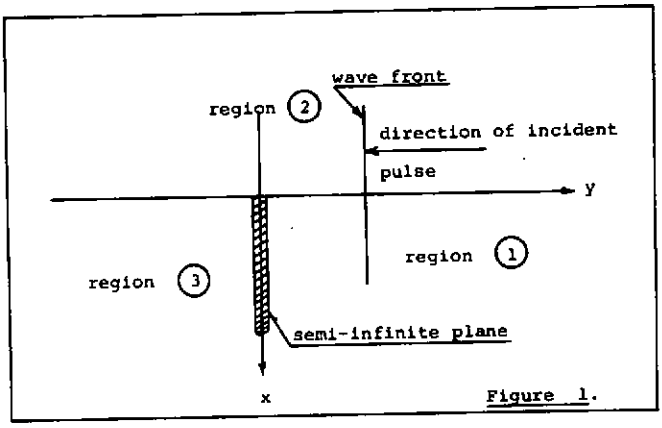

Figure 1.

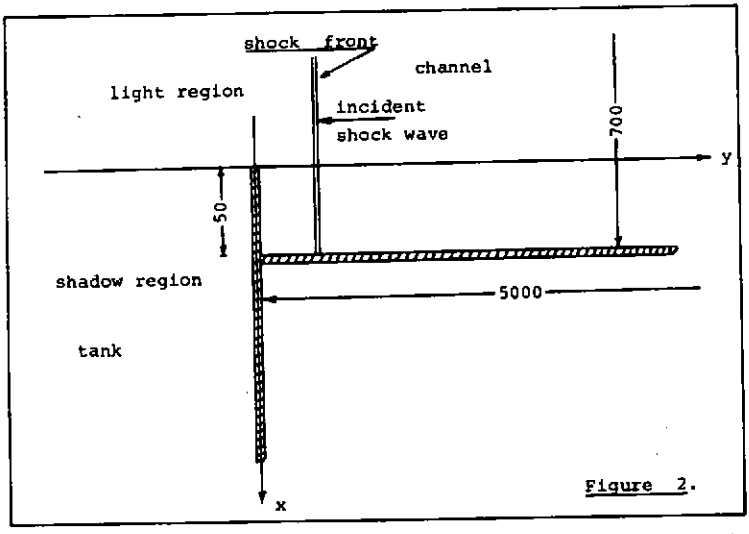

Figure 2.

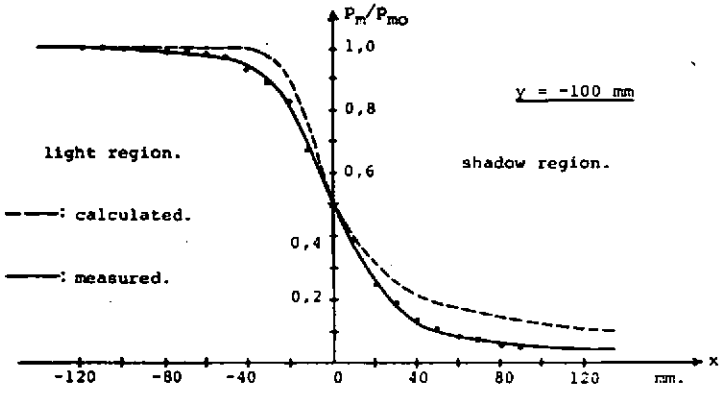

Figure 3.
Variation in peak pressure across the shadow boundary.

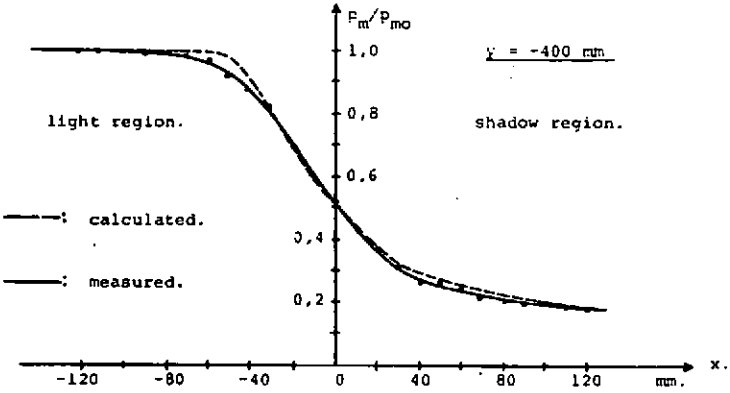

Figure 4.
Variation in peak pressure across the shadow boundary.

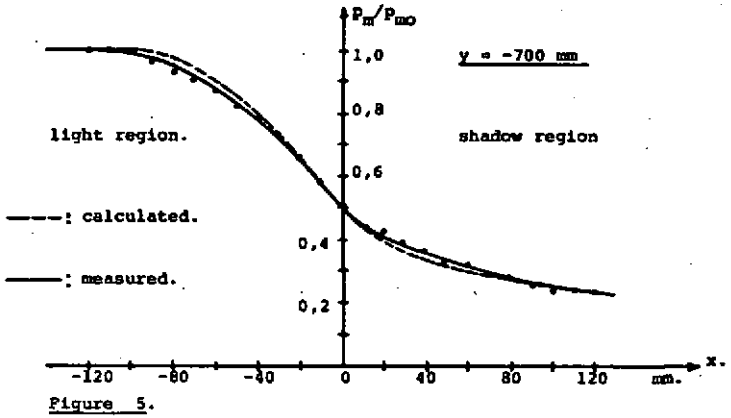

Figure 5.

Variation in peak pressure across the shadow boundary.

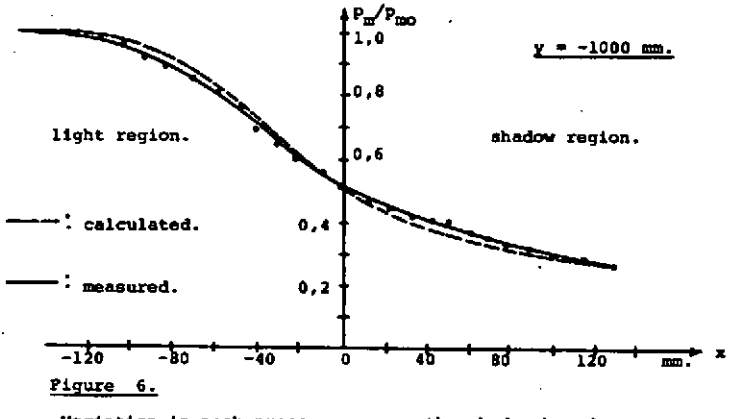

Figure 6.

Variation in peak pressure across the shadow boundary.

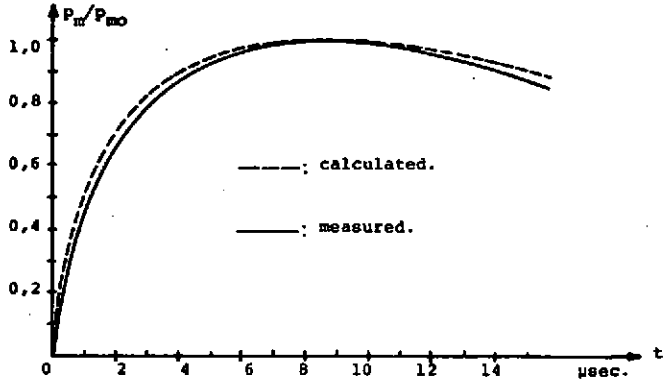

Figure 7.

Pressure-time curves measured and calculated in the point: (x,y) = (50 mm, -100 mm).

References.

[1] Sommerfeld, A., Mathematische Theorie der Diffraction. Math.Ann. 47 p.317 - 74, 1896.

[2] Sommerfeld, A., Theoretisches über die Beugung der Röntgenstrahlen. Z. Math. Phys. 46 p. 11 - 97, 1901.

[3] Lamb, H., On the diffraction of a solitary wave. Proc. Lond. Math. Soc. (2) 8 p. 422 - 37, 1910.

[4] Friedlander, F. G., The diffraction of sound pulses I - IV. Proc. Roy. Soc. A, 186 p. 322 - 67, 1946.

[5] Friedlander, F. G., Sound pulses. Cambridge University Press, 1958.

[6] Lighthill, M. J., The diffraction of blast I. Proc. Roy. Soc. A, 198 p. 454 - 70, 1949.

[7] Lighthill, M. J., The diffraction of Blast II. Proc. Roy. Soc. A, 199 p. 554 - 65, 1950.

[8] Whitham, G. E., A new approach to problems of shock dynamics I. Two-dimensional problems. Journal of Fluid Mechanics, vol. 2, part 2, p. 145 - 71, 1957.

[9] Lamb, H., Hydrodynamics. Cambridge University Press, 1963.

[10] Whittaker, E. T. and Watson, G. N., A course of modern analysis. Cambridge University Press, 1962.

[11] Bjørnø, L., On underwater explosions and the transmission of shock waves through foam plates immersed in water. (in Danish). Department of Fluid Mechanics, 1968.

[12] Bjørnø, L., A comparison between measured pressure waves in water arising from electrical discharges and detonation of small amounts of chemical explosives. Trans. ASME, Vol. 92, Ser. B, No. 1, p. 29 - 35, Feb. 1970.

NOTATION.

c : Wave velocity ∿ shock velocity ∿ sound velocity.

p : Pressure function, (index: 1,2,3 refer to regions on fig.1).

p_o : Pressure function by the incident pulse.

p_m : Peak pressure by the shock wave after diffraction.

p_{mo} : Peak pressure of the incident shock wave before diffraction.

t : Time.

T : Substitution $\left[= ct - (x^2 + y^2)^{\frac{1}{2}}\right]$

u : Substitution $\left[= z - \zeta^2\right]$

x : Coordinate in the cartesian coordinate system figure 1.

X_1 : Substitution $\left[= (x^2 + y^2)^{\frac{1}{2}} + y\right]$

X_2 : Substitution $\left[= (x^2 + y^2)^{\frac{1}{2}} - y\right]$

y : Coordinate in the cartesian coordinate system figure 1.

z : Substitution $\left[= (ct \pm y)\right]$

z' : Substitution $\left[= \frac{ct + y}{c}\right]$ dimensionless coordinate for shock waves in water.

ξ :
η : } Coordinates in the parabolic coordinate system.

ζ : Integration variable, introduced by (5).

θ : Time constant in the exponential pressure decay behind the shock front.

ρ : Density of water.

ϕ : Velocity potential.

ψ : Substitution function, introduced by (17).

Numbers in parentheses () designate formulas in the text.
Numbers in brackets [ ] designate references at the end of the paper.